Temperature dependence of the phonon frequencies of molybdenum: a tight-binding molecular dynamics study

1999 J. Phys.: Condens. Matter 11 5455

(http://iopscience.iop.org/0953-8984/11/28/306)

J. Phys.: Condens. Matter **11** (1999) 5455–5462. Printed in the UK PII: S0953-8984(99)00901-7

Temperature dependence of the phonon frequencies of molybdenum: a tight-binding molecular dynamics study

H Haas†‡, C Z Wang†, K M Ho†, M Fähnle‡ and C Elsässer§

† Ames Laboratory and Department of Physics, Iowa State University, Ames, IA 50011, USA
‡ Max-Planck-Institut für Metallforschung, Heisenbergstraße 1, 70569 Stuttgart, Germany
§ Max-Planck-Institut für Metallforschung, Seestraße 92, 70174 Stuttgart, Germany

Received 12 January 1999

Abstract. The phonon dispersion curves of molybdenum at zero temperature as well as at elevated temperatures are studied, using our recently developed semi-empirical tight-binding model. At zero temperature the phonon dispersion curves are obtained by frozen-phonon calculations as well as by a dynamical matrix approach. The phonon frequency shifts due to an increase in temperature are calculated by molecular dynamics (MD) simulations and the quasiharmonic contribution to the total frequency shift is determined. An alternative approach for calculating the frequency shifts without performing MD simulations is also presented.

1. Introduction

The low-temperature phonon spectrum of body-centred cubic (bcc) molybdenum as measured in inelastic neutron scattering experiments [1–3] exhibits a variety of anomalies: besides a depression near the symmetry point H and a depression of the $[0\xi\xi]\mathrm{T}_2$ branch at N, the longitudinal $[\xi\xi\xi]$ branch does not display the rounded dip near $\boldsymbol{q} = \frac{2}{3}[111]$ which is typical for 'regular' monatomic bcc metals (like, for instance, alkali metals [4]). These anomalies which have been attributed to the electronic features of Mo [5, 6], tend to be less pronounced at elevated temperatures [3].

Theoretical investigations of the temperature dependence of the phonon frequencies of Mo have so far been restricted to a small temperature range due to their perturbational nature [7]. In order to calculate phonon properties at higher temperatures, non-perturbative techniques such as molecular dynamics (MD) simulations are desirable. Because of the apparent influence of the electronic structure on the vibrational properties of Mo, it is necessary to use a quantum mechanical description for the interatomic force calculation in the MD simulations. Furthermore, a computationally efficient force calculation scheme is needed in order to be able to handle a large enough number of atoms over a sufficiently long period of simulation time. All of these considerations point towards the use of semi-empirical methods which take into account the quantum mechanical effects of bonding while being far less time-consuming than *ab initio* methods.

Recently, we have developed an environment-dependent tight-binding (TB) parametrization for molybdenum whose results for bulk, point defect, and surface properties at $T = 0$ K are in good agreement with *ab initio* and experimental data [8]. One of the purposes of this paper is to check whether this TB model can also be used to predict temperature-dependent properties of molybdenum and to demonstrate the feasibility of MD simulations using the

0953-8984/99/285455+08$30.00

environment-dependent TB parametrization for transition metals. To this end, we have implemented the TB model in a 'conventional' MD simulation code and compared the so-obtained phonon frequencies at elevated temperatures with those obtained by inelastic neutron scattering experiments.

Another purpose of this paper is to explore a methodically different approach for the phonon frequency calculation at elevated temperatures. If successful, it would speed up the calculation of temperature-dependent properties considerably compared to 'conventional' MD simulations.

We start in section 2 with a description of the zero-temperature phonon spectrum, which has been calculated by frozen-phonon calculations as well as by a dynamical matrix approach [4]. In section 3 we discuss technical details of the MD simulations and compare the MD results for the temperature-dependent phonon frequencies with experimental data. In section 4 we describe our alternative approach used for the calculation of the temperature dependence of the phonon frequencies and compare the results obtained from the various theoretical methods. A concluding discussion is given in section 5.

2. Phonon properties at zero temperature

As mentioned in the introduction, we will use our recently developed TB model for molybdenum for the energy and interatomic force calculations. Details concerning the functional form and fitting procedures can be found in reference [8]. The use of an environment-dependent parametrization for the elements of the Hamiltonian matrix as well as the repulsive potential provides for a good transferability of the TB parameters in our model. Applying the Hellmann–Feynman theorem, interatomic forces can be calculated easily within the framework of semi-empirical TB models (see, for instance, reference [9]).

Before applying the TB model in more extensive MD calculations, we first examined the phonon properties at zero temperature using frozen-phonon calculations. We used three different supercells for phonon modes with wavevectors along the $[\xi 00]$, $[\xi\xi 0]$, and $[\xi\xi\xi]$ directions. The supercells were stretched along the respective wavevectors to enable them to accommodate the displacement pattern of long-wavelength phonons. The supercells contained 16 atoms in the case of wavevectors along $[\xi 00]$ and $[\xi\xi 0]$, and 24 atoms for wavevectors along $[\xi\xi\xi]$. The sizes of these supercells are small enough that we could afford to use as many $\boldsymbol{k}$-points for the Brillouin zone sampling as were necessary to obtain converged phonon frequencies, except for the H-point phonon (for the problems involved in the calculation of the H phonon in Mo, see, for instance, reference [10]). With these supercells, phonons with wavevectors $\boldsymbol{q} = \frac{2\pi}{a}(\frac{n}{8}, 0, 0)$, $\frac{2\pi}{a}(\frac{n}{16}, \frac{n}{16}, 0)$, and $\frac{2\pi}{a}(\frac{n}{12}, \frac{n}{12}, \frac{n}{12})$ are accessible, with a and n standing for the lattice constant and an integer, respectively. The results are displayed in figure 1, together with the results of inelastic neutron scattering experiments at room temperature [11]. Despite some minor discrepancies, all of the phonon anomalies mentioned in the introduction are well reproduced by the TB model.

We have also used a dynamical matrix approach (see, for instance, reference [4]) for the calculation of the phonon frequencies: a cubic $5 \times 5 \times 5$ unit cell (250 atoms) was used to calculate the force constant matrix by displacing the atom at the centre of the supercell and calculating the resulting forces on all of the other atoms of the supercell. The phonon frequencies can then be calculated by diagonalizing the dynamical matrix which is the Fourier transform of the force constant matrix. The resultant phonon spectrum is very similar to the one obtained by frozen-phonon calculations except at the H point, as one can see from the comparison in figure 2. Non-negligible discrepancies indicate the presence of long-range interactions in Mo: all of the interactions are exactly taken into account by frozen-phonon-type

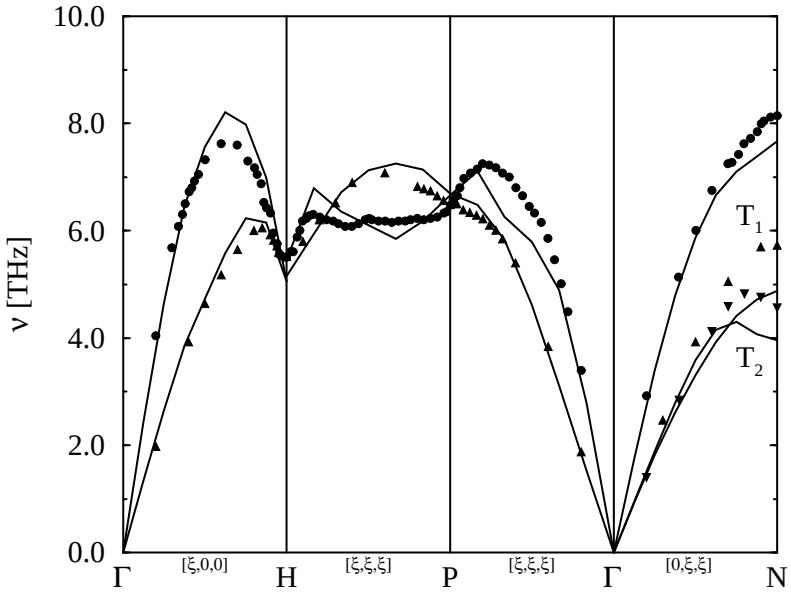

Figure 1. Comparison of the phonon frequencies in bcc Mo derived from the TB method (solid curves) and from inelastic neutron scattering (reference [11]) at $T = 296$ K. The dots and triangles represent the experimental data for longitudinal and transverse modes respectively.

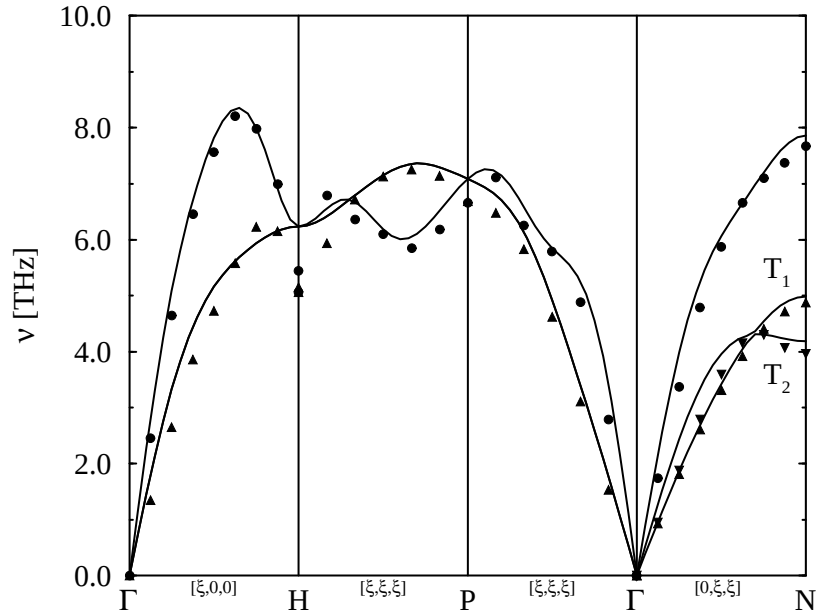

Figure 2. Comparison of the phonon frequencies in bcc Mo derived from the TB calculations using the dynamical matrix method (solid curves) and the frozen-phonon method (dots and triangles represent longitudinal and transverse modes respectively).

calculations. The dynamical matrix calculations, however, are subject to finite-size effects, and physically meaningful interactions can be calculated only up to a certain interatomic distance

depending on the size of the supercell (in our case, we neglected interactions beyond ninth-nearest-neighbour interactions). In table 1 we have listed the non-vanishing elements of the force constant matrix. Comparison with the force constants determined by a direct fit of a Born–von Kármán model to the experimental phonon spectrum [11] reveals good agreement for the first two neighbour shells, but there are considerable discrepancies for larger interatomic distances. This indicates that, for the case of long-range interactions, the force constants are not uniquely determined by the fit to the experimental phonon spectrum. One can change the values, especially of the long-range force constants, and keep the shape of the phonon spectrum nearly unchanged. Another interesting feature is the relatively large values for the fifth-nearest-neighbour force constants; this has been attributed to the fact that a fifth-nearest-neighbour pair of atoms in a bcc crystal is coupled by two nearest-neighbour bonds [12].

Table 1. Force constants obtained by the TB model and by fitting a Born–von Kármán model directly to the experimentally measured phonon spectrum [11]. The Greek indices label the Cartesian coordinates of the nth-nearest-neighbour force constant.

$n\kappa\kappa'$	TB (N m^{-1})	Fit (N m^{-1})	$n\kappa\kappa'$	TB (N m^{-1})	Fit (N m^{-1})
1xx	17.37	16.51	7xx	0.53	0.29
1xy	10.70	11.78	7xy	0.87	−0.16
2xx	42.57	44.57	7xz	0.04	−0.06
2yy	−4.04	−2.69	7zz	−0.05	−0.75
3xx	1.53	3.60	8xx	−0.20	
3xy	−1.35	1.72	8yy	−0.05	
3zz	−5.15	0.69	8zz	−0.30	
4xx	−3.99	−2.65	8xy	−0.33	
4xy	−0.87	0.26	9xx	1.75	
4yy	0.45	−0.43	9yy	0.12	
4yz	1.29	0.71	9xy	0.75	
5xx	4.03	0.57	9yz	−0.30	
5xy	5.26	0.69			
6xx	1.00	3.97			
6yy	0.40	0.85			

3. Molecular dynamics simulation

The MD simulations were performed under microcanonical conditions using a cubic $3 \times 3 \times 3$ unit cell (54 atoms) with periodic boundary conditions. The lattice constant was scaled according to the experimentally measured thermal expansion coefficients (the linear and quadratic thermal expansion coefficients are 3.879×10^{-6} K^{-1} and 1.842 K^{-2} respectively) [13]. After assigning each atom a random displacement from its perfect bcc position, the velocities were scaled for several hundred time steps in order to achieve the desired temperature. Thereafter, the temperature control was turned off and the simulation continued for several hundred time steps before MD data were recorded for later analysis. The phonon frequencies were calculated by taking the Fourier transform of the velocity–velocity autocorrelation function [14]

$$G(\boldsymbol{q},\omega) = \int \mathrm{d}t\ \mathrm{e}^{\mathrm{i}\omega t} \sum_n \mathrm{e}^{-\mathrm{i}\boldsymbol{q}\cdot\boldsymbol{R}_n} \frac{\langle \boldsymbol{v}_n(t)\cdot\boldsymbol{v}_0(0)\rangle}{\langle \boldsymbol{v}_n(0)\cdot\boldsymbol{v}_0(0)\rangle} \tag{1}$$

with $\boldsymbol{v}_n(t)$ and $\boldsymbol{R}_n$ being the velocity at time t and the ideal bcc lattice position of atom n. The wavevector $\boldsymbol{q}$ has to be commensurate with the MD box, which, in our case, translates

into six non-equivalent wavevectors $\boldsymbol{q} = \frac{2\pi}{a}(\frac{1}{3}, 0, 0)$, $\frac{2\pi}{a}(\frac{2}{3}, 0, 0)$, $\frac{2\pi}{a}(1, 0, 0)$, $\frac{2\pi}{a}(\frac{1}{3}, \frac{1}{3}, 0)$, $\frac{2\pi}{a}(\frac{1}{3}, \frac{1}{3}, \frac{1}{3})$, and $\frac{2\pi}{a}(\frac{2}{3}, \frac{2}{3}, \frac{2}{3})$. In order to get better statistics, we took the average over the star of $\boldsymbol{q}$.

In order to check our MD code, we performed a low-temperature MD simulation at $T = 10$ K, using a time step of 2.86×10^{-15} s and four $\boldsymbol{k}$-points [15] for the band-structure energy and force calculation. We ran 2048 MD steps, corresponding to a total simulation time of 5.9 ps. The phonon frequencies obtained by taking the average of $G(\boldsymbol{q}, \omega)$ agreed very well with those obtained from frozen-phonon-type calculations using the same supercell and $\boldsymbol{k}$-point mesh.

To check the convergence of the MD results with respect to the number of $\boldsymbol{k}$-points used for the force and energy calculation, we have compared the phonon frequencies obtained via frozen-phonon calculations using the above-mentioned 54-atom supercell and four $\boldsymbol{k}$-points with those obtained via frozen-phonon calculations using smaller supercells which are stretched along the direction of the phonon wavevector in order to accommodate long-wavelength phonons. For the latter supercells we can afford to use as many $\boldsymbol{k}$-points for the Brillouin zone sampling as are necessary in order to obtain converged results (see reference [8]). Since the phonon frequencies obtained by using these different supercells and $\boldsymbol{k}$-point meshes differ considerably (by much as 0.7 THz for certain phonon modes), we cannot consider our low-temperature MD results as being converged if only four $\boldsymbol{k}$-points are used.

On the other hand, we have performed high-temperature ($T = 1200$ K) MD simulations using two different $\boldsymbol{k}$-point meshes containing 4 and 32 $\boldsymbol{k}$-points† and a time step of 0.72×10^{-15} s. We used 16 384 MD steps, corresponding to a total simulation time of 11.7 ps. The so-obtained frequencies turned out to be in very good agreement (better than ± 0.1 THz for all phonon modes), implying that four $\boldsymbol{k}$-points are sufficient in order to get converged results in high-temperature simulations. This finding may be explained by the fact that an increase in temperature will lead to a smearing out of the Fermi surface due to the thermal motion of the atoms and fewer $\boldsymbol{k}$-points are needed for the Brillouin zone sampling in order to take into account the details of the Fermi surface which are present at low temperatures.

In order to obtain meaningful frequency shifts, which can be compared to experimental results, the numbers appearing in table 2 were calculated by subtracting the frequencies obtained by $T = 0$ K frozen-phonon calculations with converged $\boldsymbol{k}$-point sampling from those obtained by the $T = 1200$ K, four-$\boldsymbol{k}$-point MD simulation.

In the quasiharmonic approximation, the temperature dependence of the phonon frequencies is solely due to the effect of thermal expansion; hence phonon–phonon interactions are neglected. In order to study the quasiharmonic contribution to the total frequency shift as obtained by our MD simulations, we performed frozen-phonon calculations at exactly the same lattice constants as those used in our high-temperature MD simulations, and the same 54-atom supercell. For these calculations we have used enough $\boldsymbol{k}$-points to ensure convergence. The results can be seen in table 2. Obviously, the quasiharmonic contributions to the total frequency shift vary for different phonon modes.

4. An alternative approach

Running a conventional MD simulation using a semi-empirical TB scheme for the force calculation still represents a time-consuming undertaking, particularly if one needs to be concerned about using enough $\boldsymbol{k}$-points to ensure the convergence of the results. Therefore, it

† The 32 K-points consist of $K_1 = \frac{2\pi}{L}(\frac{1}{8}, \frac{1}{8}, \frac{1}{8})$, $K_2 = \frac{2\pi}{L}(\frac{3}{8}, \frac{1}{8}, \frac{1}{8})$, $K_3 = \frac{2\pi}{L}(\frac{3}{8}, \frac{3}{8}, \frac{1}{8})$, $K_4 = \frac{2\pi}{L}(\frac{3}{8}, \frac{3}{8}, \frac{3}{8})$ and their stars under the cubic symmetry. L is the dimension of the cubic supercell used in the simulations.

Table 2. The frequency shift (THz) for an increase of temperature from 295 K to 1203 K (experiment) and from 0 K to 1200 K (TB calculations). The TB results represent the frequency shifts calculated by using equation (1) (MD), assuming the quasiharmonic approximation (QH) and performing frozen-phonon calculations on the configurations generated by equation (2) (CA).

		Tight binding		
Mode	Experiment	MD	QH	CA
$\frac{2\pi}{a}(\frac{1}{3},0,0)$L	−0.34	−0.28	−0.28	−0.24
$\frac{2\pi}{a}(\frac{1}{3},0,0)$T	−0.11	−0.16	−0.13	−0.17
$\frac{2\pi}{a}(\frac{2}{3},0,0)$L	−0.54	−0.70	−0.32	−0.58
$\frac{2\pi}{a}(\frac{2}{3},0,0)$T	−0.10	−0.68	−0.29	−0.62
$\frac{2\pi}{a}(1,0,0)$	+ 0.20	−0.21	−0.26	−0.09
$\frac{2\pi}{a}(\frac{1}{3},\frac{1}{3},0)$L	−0.32	+ 0.05	−0.34	+ 0.01
$\frac{2\pi}{a}(\frac{1}{3},\frac{1}{3},0)T_1$	−0.50	−0.37	−0.22	−0.43
$\frac{2\pi}{a}(\frac{1}{3},\frac{1}{3},0)T_2$	−0.21	−0.46	−0.20	−0.27
$\frac{2\pi}{a}(\frac{1}{3},\frac{1}{3},\frac{1}{3})$L	−0.27	−0.23	−0.39	−0.15
$\frac{2\pi}{a}(\frac{1}{3},\frac{1}{3},\frac{1}{3})$T	−0.47	−0.46	−0.24	−0.46
$\frac{2\pi}{a}(\frac{2}{3},\frac{2}{3},\frac{2}{3})$L	−0.65	−0.86	−0.25	−0.64
$\frac{2\pi}{a}(\frac{2}{3},\frac{2}{3},\frac{2}{3})$T	−0.33	−0.31	−0.32	−0.19

would be highly desirable to have an alternative method for calculating the phonon frequencies at non-zero temperatures without actually running MD simulations. In this section, we will investigate an approach based on an ensemble average scheme which would render MD simulations altogether needless, and thus reduce computation time considerably.

This attempt consists of three steps:

(a) Generate an ensemble of atomic configurations according to a well-defined recipe, which can be thought of as taking snapshots during the course of a regular MD simulation at a given temperature.

(b) Perform frozen-phonon calculations on each configuration, by assigning to each atom a displacement vector according to the phonon mode under investigation in addition to the displacement from the ideal bcc position due to thermal movement.

(c) Take the average of the so-obtained phonon frequencies.

The recipe for generating the atomic configurations is as follows. We describe the thermal displacement of each atom n by a displacement vector $\boldsymbol{u}_n$ from its ideal bcc lattice position $\boldsymbol{R}_n$, given by

$$\boldsymbol{u}_n = \sum_{\boldsymbol{q}\lambda} u_{\boldsymbol{q}\lambda}(T)\boldsymbol{e}_{\boldsymbol{q}\lambda}\exp(\mathrm{i}(\boldsymbol{q}\cdot\boldsymbol{R}_n + \delta_{\boldsymbol{q}\lambda})) \tag{2}$$

where $\boldsymbol{e}_{\boldsymbol{q}\lambda}$ stands for the normalized eigenvector of phonon mode $\boldsymbol{q}\lambda$ with $\boldsymbol{q}$ and λ denoting the wavevector and polarization, respectively. The sum runs over all phonon modes $\boldsymbol{q}\lambda$ which are commensurate with our 54-atom supercell. The so-obtained configurations can be conceived as superpositions of frozen phonons with $\delta_{\boldsymbol{q}\lambda}$ chosen randomly. The temperature enters via a temperature-dependent displacement amplitude $u_{\boldsymbol{q}\lambda}(T)$ which has been calculated according

to

$$u_{q\lambda}(T) = \sqrt{\frac{k_B T}{m\omega_{q\lambda}^2}}. \tag{3}$$

The anharmonicity of the potential was taken into account by displacing the atoms both in positive and negative directions and taking the average over the energy differences of these two calculations. The numbers appearing in table 2 represent again the averages over at least 50 configurations. Performing frozen-phonon calculations on an ensemble of configurations obtained by actually saving configurations during the course of an MD simulation results in similar values for the phonon frequencies, which justifies the use of equation (2).

5. Discussion

First, we compare the frequency shift calculated via the velocity–velocity autocorrelation function with the ones obtained by inelastic neutron scattering. As one can see from table 2, the overall tendency observed in inelastic neutron scattering experiments, namely the weakening of the phonon anomalies as the temperature increases, is very well reproduced by the MD results. A frequency shift at elevated temperatures can be attributed basically to three different mechanisms:

(a) Thermal expansion will lead to a change of force constants and hence to a change in phonon frequencies. This *quasiharmonic* contribution to the total frequency shift has been calculated in the previous section.
(b) Another contribution comes from anharmonic phonon–phonon interactions which become more important as the temperature increases.
(c) Finally, non-adiabatic and many-body effects which are beyond the scope of the local density approximation (LDA) may contribute to a frequency shift [16].

The effects of lattice expansion as well as anharmonic phonon–phonon interactions are taken into account by the MD simulations, whereas non-adiabatic and many-body effects are not included, since our model is based on LDA calculations. Non-negligible differences between the experimentally observed frequency shifts and the MD results may hence be interpreted as a strong hint that those effects may play an important role in Mo.

When comparing the results obtained by means of conventional MD simulations via the velocity–velocity autocorrelation function with those obtained by performing frozen-phonon calculations on configurations created by using equation (2), one has to be well aware of the fact that these results are converged only up to ± 0.1 THz with respect to the number of $\boldsymbol{k}$-points used for the Brillouin zone sampling. Thus, the agreement of the frequency shifts obtained by the two different techniques is satisfactory. However, if the absolute frequency shift is of about the same order of magnitude as the uncertainty due to the use of a limited number of $\boldsymbol{k}$-points, it might become necessary to use a denser grid of $\boldsymbol{k}$-points.

Acknowledgments

Ames Laboratory is operated for the US Department of Energy by Iowa State University under contract No W-7405-Eng-82. This work was supported by the Director for Energy Research, Office of Basic Energy Sciences, and the High Performance Computing and Communications initiative, including a grant of computer time at the National Energy Research Supercomputing Center. One of the authors (HH) acknowledges financial support from the Deutscher Akademischer Austauschdienst.

References

[1] Woods A D B and Chen S H 1964 *Solid State Commun.* **2** 233
[2] Powell B M, Martel P and Woods A D B 1968 *Phys. Rev.* **171** 727
[3] Zarestky J, Stassis C, Harmon B N, Ho K-M and Fu C L 1983 *Phys. Rev.* B **28** 697
[4] Frank W, Elsässer C and Fähnle M 1995 *Phys. Rev. Lett.* **74** 1791
[5] Varma C M and Weber W 1979 *Phys. Rev.* B **19** 6142
[6] Ho K-M, Fu C-L and Harmon B N 1983 *Phys. Rev.* B **28** 6687
[7] Ye Y Y, Ho K M, Chen Y and Harmon B N 1991 *J. Phys.: Condens. Matter* **3** 9629
[8] Haas H, Wang C Z, Fähnle M, Elsässer C and Ho K-M 1998 *Phys. Rev.* B **57** 1461
[9] Wang C Z, Chan C T and Ho K M 1989 *Phys. Rev.* B **39** 8586
[10] Buck S, Hummler K and Fähnle M 1996 *Phys. Status Solidi* b **195** K9
[11] Powell B M, Martel P and Woods A D B 1977 *Can. J. Phys.* **55** 1601
[12] Finnis M W, Kear K L and Pettifor D G 1984 *Phys. Rev. Lett.* **52** 291
[13] Waseda Y, Hirata K and Ohtani M 1975 *High Temp.–High Pressures* **7** 221
[14] Wang C Z, Chan C T and Ho K M 1990 *Phys. Rev.* B **42** 11 276
[15] The four K-points used in the simulation consist of $K_1 = \frac{2\pi}{L}(\frac{1}{4}, \frac{1}{4}, \frac{1}{4})$ and its star under the cubic symmetry. L is the dimension of the cubic supercell used in the simulations.
[16] Fu C L, Ho K M, Harmon B N and Liu S H 1983 *Phys. Rev.* B **28** 2957